

Helmut Gärtner  
Arbeitsgruppe Metallphysik,  
Fachbereich Physik  
Gesamthochschule Kassel

## PHYSICAL PROPERTIES OF TECHNICAL SURFACES

### I. Introduction

In recent years a variety of new physical methods has been developed in order to modify technical surfaces. The reason for these activities are, besides the production of decorative coatings, to increase wear resistance and to reduce corrosion. The leading idea in this field is to work with compound systems in which the basic material is responsible for solidity and stiffness of the samples and the surface layers take care of wear and corrosion protection.

Besides ion implantation, which is the subject of this conference, ion plating is a very suitable method in the area of surface modification of metals by deposition of surface coatings. In order to illustrate the potential of this technique we shall discuss in this contribution the influence of ion plated copper layers on titanium in cold impact extrusion experiments.

### II. Ion Plating

Ion plating was invented in 1963 by Mattox /1/. In a sense it is the addition of two well known processes: evaporation and sputtering. Fig. 1. (taken from /2/) shows the three processes schematically. From the physical point of view the important difference between these methods is the energy of the atoms or ions when they reach the substrate. For evaporation this energy ranges from 0,1 to 1 eV. In d.c. sputtering the upper limit of the

energy involved is in the range of 30 eV while with ion plating it can go up to the order of thousand eV.

A typical d.c. ion plating apparatus consists of a bell jar with an evaporation source and a watercooled substrate which acts as the cathode as shown in Fig. 1 (c). First the jar is evacuated to a pressure of about  $10^{-5}$  mbar, then in a flowing gas, argon for instance at  $10^{-2}$  mbar, a discharge is struck between the earthed source and the substrate cathode. In this glow discharge the metal substrate is carefully sputter-cleaned. After a while the material to be deposited on the sample at the cathode is evaporated in to the plasma. The evaporated atoms will be partly ionized, scattered by the gas ions and accelerated towards the cathode where they are deposited. During the deposition the sputtering continues to remove any material from the substrate which is not tightly bonded. Due to the ion bombardment the temperature of the sample may easily rise up to about 300 °C favouring diffusion processes which enhance the adhesion of the deposited films too.

The ion plating rig used in the experiments to be described in this paper is shown in Fig. 2. It is a conventional d.c. diode arrangement. The water cooled cathode has 12 cm diameter; the distance between the evaporation source (tungsten filament) and the cathode is 21 cm. The base pressure reached with an oil diffusion pump is  $10^{-5}$  mbar, the operating pressure is  $10^{-2}$  mbar. The negative d.c. bias at the cathode is up to 6,5 kV. Under typical discharge conditions we obtain a current density of 0,9 mA/cm<sup>2</sup> at the cathode.

### III. The Titanium-Copper-System

Titanium and its alloys are materials of increasing importance in e.g. aerospace and chemical industries. Pure titanium combines low density (4,51 g/cm<sup>3</sup>) with a high melting point (1963 K) and high tensile strenght (300 - 750 N/mm<sup>2</sup>). As its price and production costs are high the waste of material by conventional machining processes is to be avoided. Economical machining processes such as cold forging, and, especially, cold impact extrusion are highly desired as metal forming processes without loss of

material during the production of desired components.

Because of the high pressures (up to  $2000 \text{ N/mm}^2$ ) involved in these forming processes one must be aware of sticking and cold welding. In order to avoid these difficulties one can protect the tools /3/ or one has to develop a lubrication system which is able to separate the titanium from the steel tools. In spite of some efforts in the fifties and sixties it turned out to be difficult, to find a coating system and lubricant to meet the tribological requirements of the cold impact extrusion of titanium and its alloys. As a consequence of this the general introduction of the cold forging of titanium into production engineering did not take place.

The samples used in this study were titanium cylinders of technical grade pure material (diameter 30,4 mm, height 25 mm). All samples were degreased with trichlorethylene in an ultrasonic cleaner prior to mounting in the ion plating rig described above. Copper coatings with thicknesses up to  $5 \mu\text{m}$  were deposited in an argon atmosphere. The extrusion tests were performed on a hydraulic press with a nominal force of 1000 kN /4, 5/. As Fig. 3. shows the best results, minimum friction, were obtained with copper coatings between 1 and  $2 \mu\text{m}$ . Even in the case of backward extrusion (cupping) where the highest forming forces were employed the adhesion between the copper films and titanium cylinders was perfect. The inner surfaces of the cups were smooth and shiny after the severe forming process without any traces of sticking or cold welding.

#### IV. Residual stress analysis

In further studies into the nature of these copper layers the preparation parameters (process gas and deposition rate) were varied /6/. For this purpose titanium strips (60 mm x 19 mm x 1 mm) were cut from 99,8 % pure titanium (TIKRUTAN RT 12, Krupp-Klöckner G.m.b.H., Essen). The deposition rate was 2 nm/s and 1 nm/s for argon (99,9999 %) and 4 nm/s and 2 nm/s for nitrogen (99,9995 %).

In order to simulate the severe loads that the copper layers on titanium cylinders undergo during cold extrusion, part of the ion plated strips were drawn on a tensile testing machine. The strain was about  $\epsilon = 25 \%$ . The tensile

strength was  $375 \text{ N/mm}^2$  for the untreated titanium samples. It reduced to  $345 \text{ N/mm}^2$  for the ion plated samples.

The residual stresses of all layers were examined by X-rays. A Siemens Kristalloflex 4 diffractometer was equipped with a special tilting head in order to provide a  $\psi$ -diffractometer /7/. Fig. 4. shows the scattering geometry. The scattered intensities of the nickel-filtered  $\text{CuK}\alpha$ -radiation were strip chart recorded with a scintillation counter. The Bragg angles  $2\theta_0$  employed were  $136,55^\circ$  and  $144,77^\circ$ , which correspond to the the (331) and (420) lattice planes respectively in copper. The copper peaks are well separated from the neighbouring titanium peaks, which are also recorded. From the change in peak intensity with changing tilting angle it may be concluded that a certain amount of texture and lattice inhomogeneities exists in the copper layers. In some cases the copper peak can be made to vanish by changing  $\psi$  only about  $6^\circ$ .

In X-ray analysis of residual stresses the shifts  $\Delta\theta$  of the Bragg angle caused by changes in the lattice plane spacings  $d$  due to internal or external stresses are measured. According to Glocker /8/ the following relation holds:

$$\frac{\Delta d}{d} = -\cotan \theta_0 \cdot \Delta\theta. \quad (1)$$

The change in the lattice constant is attributed to uniform strains in the surface, which correspond to a biaxial stress tensor ( $\sigma_3 = 0$  perpendicular to the surface). In the scattering geometry, as defined by Fig. 4., one has

$$c_{\varphi\psi} = \frac{1}{2} s_2 \sigma_{\varphi} \sin^2 \psi + s_1 (\sigma_1 + \sigma_2) \quad (2)$$

with

$$\sigma_{\varphi} = \sigma_1 \cos^2 \varphi + \sigma_2 \sin^2 \varphi. \quad (3)$$

$s_1, s_2$  are the Voigt elastic constants. By varying  $\varphi$  and  $\psi$ ,  $\sigma_1$  and  $\sigma_2$  can be determined.

For polycrystalline material with an isotropic distribution of the crystallites the linear relationship given in eqn. (2) is obeyed. It is well-known /9/ that perturbations such as textures and stress gradients give non-linear

$c$  versus  $\sin^2\psi$  curves. We nevertheless use eqn. (2) in order to gain some understanding of the behaviour of the different copper layers.

The results of our measurements are collected together in Fig. 5. A  $\phi$  value of  $45^\circ$  was commonly employed. The axis intercept at  $\sin^2\psi = 0$  might be in error since it is very sensitively affected by a possible maladjustment of the scattering angle  $\theta$  in the goniometer. Therefore, only the slope of the straight lines is reliable. From this slope we deduce an effective stress, which describes the true stresses, but also includes other lattice disturbances. The values of the effective stresses are summarized in the following table:

gas, deposition rate	$\sigma_\psi$ (undrawn) N/mm <sup>2</sup>	$\sigma_\psi$ (drawn) N/mm <sup>2</sup>
Ar, fast	152	-134
Ar, slow	452	-417
N <sub>2</sub> , fast	-103	- 73
N <sub>2</sub> , slow	-205	-208

The undrawn samples show tensile stresses for argon and compressive stresses for nitrogen. After drawing all samples show compressive stresses in agreement with measurements on copper bulk material /10, 11/. For argon the large values of the effective stresses indicate that the copper lattice is heavily disturbed.

Fig. 6. shows the influence of the process gas on the behaviour of ion plated copper layers under cold backward extrusion (cupping). Both argon and nitrogen produce satisfactory layers in ion plating. The maximum forming force for copper layers ion plated in nitrogen is slightly larger than that for layers plated in argon.

#### V. Conclusions

Physical properties of technical surfaces can be drastically modified by surface layers. Ion plating is a powerful technique to produce such layers. The high energy of the incoming particles lead to very good adhesion between the deposited film and the substrate. Even under the demanding conditions of cold

backward extrusion ion plated copper layers proved to adhere to titanium cylinders.

The experiments discussed in this contribution were performed under laboratory conditions on small samples. There remains the problem how to enlarge the ion plating rig in order to cover larger objects.

The deposition rate employed in this study was rather low. It can be increased by using a separately pumped evaporation source (e-gun). On the other hand it is not known at the moment how the quality of the deposited layers depends on the deposition rate. It might be that the excellent adhesion between the copper layers and titanium as described above is due to the relatively slow deposition rates in the ion plating process.

References

- /1/ D. M. Mattox, J. Appl. Phys. 34 (1963) 2493
- /2/ E. W. Williams, Solid State Technology, Feb. 1979 p. 80
- /3/ G. K. Wolf and H. Westheide, Mater. Sci. Eng. 69 (1985) 219
- /4/ H. Gärtner et al., Int. Tagung Verschleiß- und Korrosionsschutz durch Ionen- und plasmagestützte Vakuumbeschichtungstechnologien, TH Darmstadt, Schriftenreihe Wiss. u. Techn. 20 (1983) 199
- /5/ H. W. Wagener and K. H. Tampe, Fifth Int. Conference on Titanium, Munich, Sept. 1984
- /6/ I. Riebeling, K. Thoma and H. Gärtner, Mater. Sci. Eng. 69 (1985) 435
- /7/ U. Wolfstieg in Härtereitech. Mitt. 31 (1976) 19
- /8/ R. Glocker, Materialprüfung mit Röntgenstrahlen, Springer, Berlin-Heidelberg-New York, 1971
- /9/ V. Hauk and G. Vaessen in V. Hauk and E. Macherauch (eds.), Eigenspannungen und Lastspannungen Hanser, München (1981), p. 39
- /10/ C. O. Leiber and E. Macherauch, Z. Metallkd., 51 (1960) 621; 52 (1961) 196
- /11/ S. Karashima, R. Prümmer and E. Macherauch, Materialprüfung, 10 (1968) 262.

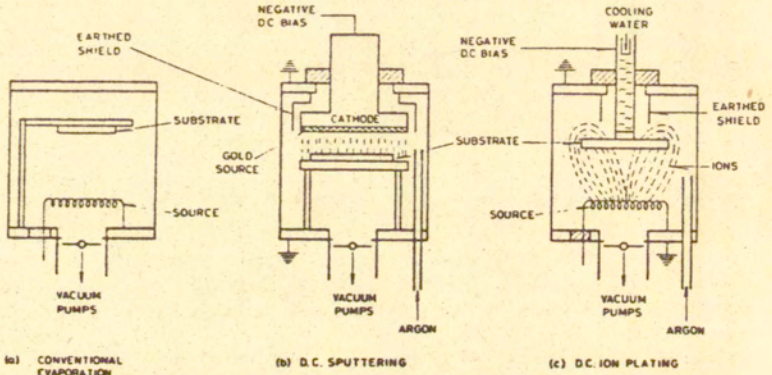


Fig. 1. Schematic comparison of three related deposition processes (taken from /2/).



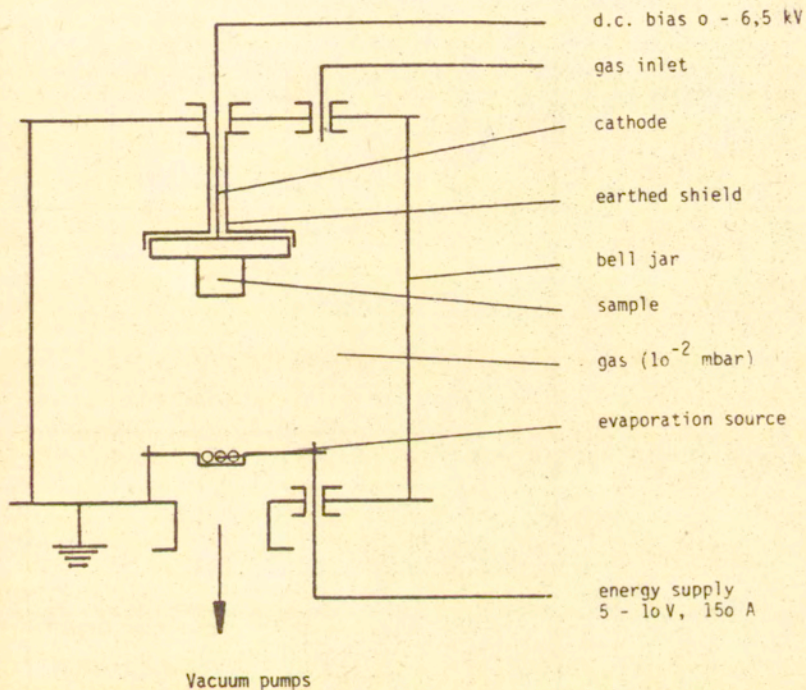


Fig. 2. Ion plating apparatus.

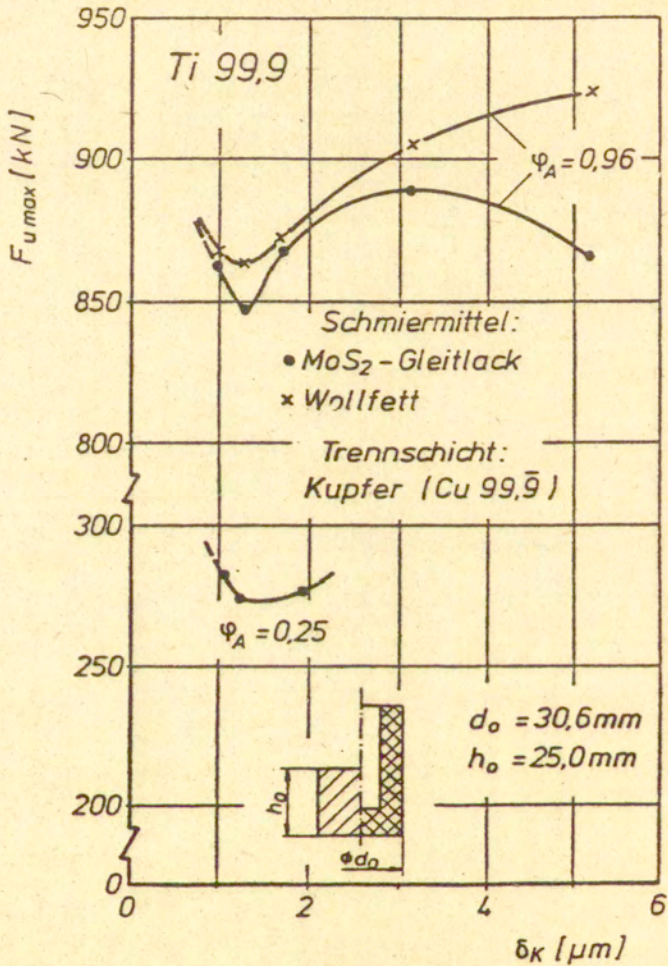


Fig. 3. Maximum forming force as a function of the thickness of the ion plated copper layers.



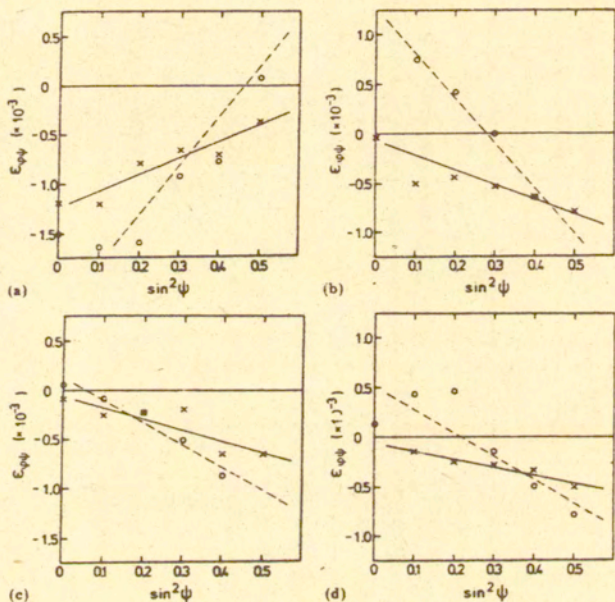


Fig. 5. Change in lattice spacing for the (420) plane (x, —, fast deposition rate; o, ---, slow deposition rate) showing the effect of drawing on the same sample: (a) argon atmosphere, undrawn; (b) argon atmosphere, drawn (thickness,  $1.1 \mu\text{m}$ ); (c) nitrogen atmosphere, undrawn; (d) nitrogen atmosphere, drawn (thickness for fast deposition rate,  $1.7 \mu\text{m}$ ; thickness for slow deposition rate,  $2.0 \mu\text{m}$ ).

(taken from /6/).

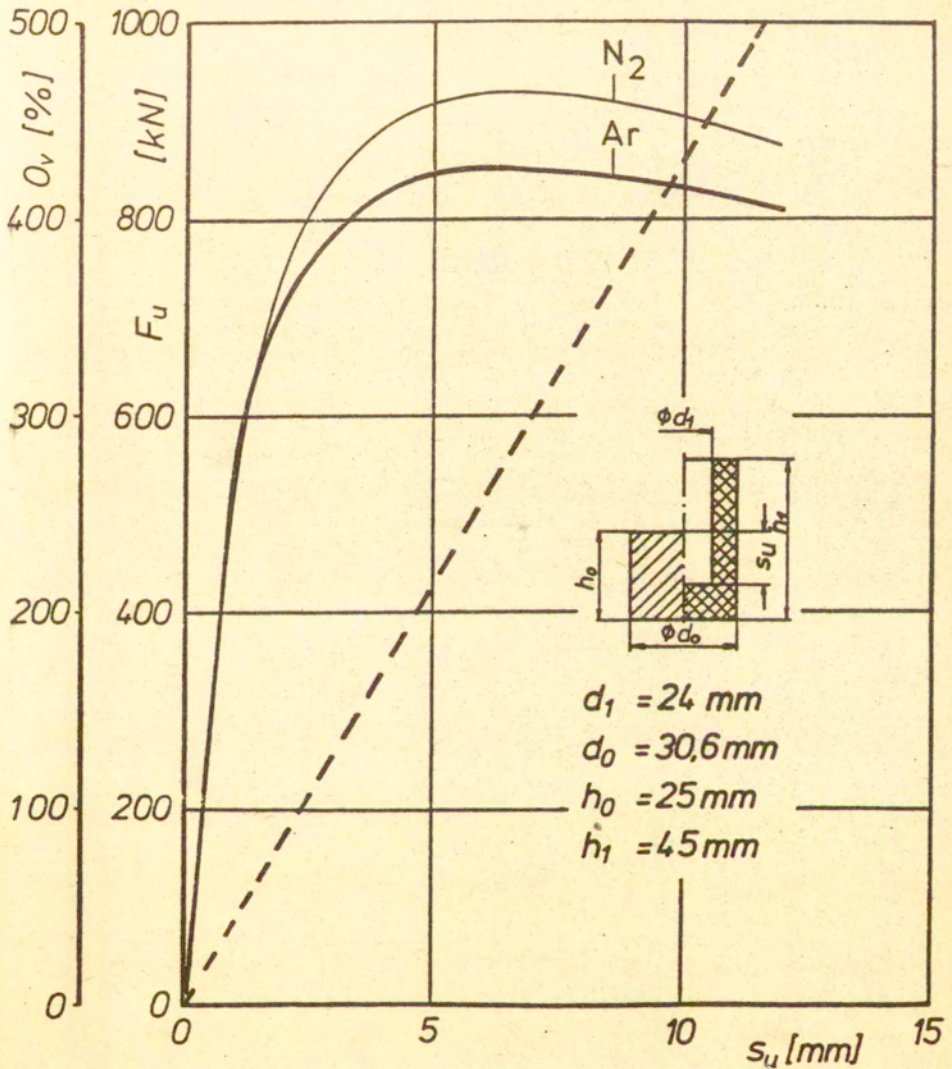


Fig. 6. Force  $F_u$  (—) and surface enlargement  $O_v$  (----) as a function of punch travel for argon and nitrogen atmospheres. The inset shows the dimensions of the cylinders used in extrusion (taken from /6/).